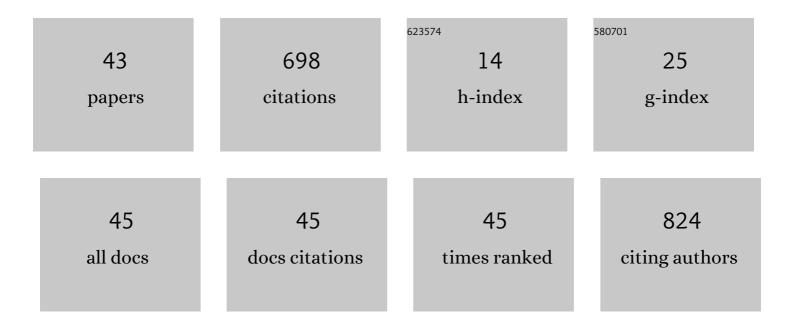
Tsutomu Nakamura

List of Publications by Year in descending order

Source: https://exaly.com/author-pdf/5034586/publications.pdf Version: 2024-02-01



#	Article	IF	CITATIONS
1	Systematic circular permutation of an entire protein reveals essential folding elements. Nature Structural Biology, 2000, 7, 580-585.	9.7	111
2	Tertiary Structure and Carbohydrate Recognition by the Chitin-Binding Domain of a Hyperthermophilic Chitinase from Pyrococcus furiosus. Journal of Molecular Biology, 2008, 381, 670-680.	2.0	59
3	Oxidation of archaeal peroxiredoxin involves a hypervalent sulfur intermediate. Proceedings of the National Academy of Sciences of the United States of America, 2008, 105, 6238-6242.	3.3	57
4	Crystal structure of peroxiredoxin from Aeropyrum pernix K1 complexed with its substrate, hydrogen peroxide. Journal of Biochemistry, 2010, 147, 109-115.	0.9	54
5	The First Crystal Structure of l-Threonine Dehydrogenase. Journal of Molecular Biology, 2007, 366, 857-867.	2.0	36
6	Circular Permutation Analysis as a Method for Distinction of Functional Elements in the M20 Loop of Escherichia coliDihydrofolate Reductase. Journal of Biological Chemistry, 1999, 274, 19041-19047.	1.6	31
7	Kinetic and crystallographic analyses of the catalytic domain of chitinase from <i>Pyrococcus furiosus</i> – the role of conserved residues in the active site. FEBS Journal, 2010, 277, 2683-2695.	2.2	30
8	Crystal structure of thioredoxin peroxidase from aerobic hyperthermophilic archaeon Aeropyrum pernix K1. Proteins: Structure, Function and Bioinformatics, 2005, 62, 822-826.	1.5	27
9	Cloning and Sequence Analysis of the Gene for Phosphoenolpyruvate Carboxylase from an Extreme Thermophile, Thermus sp1. Journal of Biochemistry, 1995, 118, 319-324.	0.9	26
10	Structure of the catalytic domain of the hyperthermophilic chitinase fromPyrococcus furiosus. Acta Crystallographica Section F: Structural Biology Communications, 2007, 63, 7-11.	0.7	24
11	Screening for Stable Mutants with Amino Acid Pairs Substituted for the Disulfide Bond between Residues 14 and 38 of Bovine Pancreatic Trypsin Inhibitor (BPTI). Journal of Biological Chemistry, 2002, 277, 51043-51048.	1.6	23
12	Expression from engineered <i>EscherichiaÂcoli</i> chromosome and crystallographic study of archaeal <i>N</i> , <i>N</i> ′â€diacetylchitobiose deacetylase. FEBS Journal, 2014, 281, 2584-2596.	2.2	22
13	Crystal structure of the cambialistic superoxide dismutase from Aeropyrum pernix K1 - insights into the enzyme mechanism and stability. FEBS Journal, 2011, 278, 598-609.	2.2	20
14	Characterization and crystal structure of the thermophilic ROK hexokinase from Thermus thermophilus. Journal of Bioscience and Bioengineering, 2012, 114, 150-154.	1.1	19
15	Expression, refolding, and purification of active diacetylchitobiose deacetylase from Pyrococcus horikoshii. Protein Expression and Purification, 2012, 84, 265-269.	0.6	15
16	Kinetic and crystallographic analyses of the catalytic domain of chitinase from Pyrococcus furiosus- the role of conserved residues in the active site. FEBS Journal, 2010, 277, 2683-2695.	2.2	13
17	Structure of peroxiredoxin from the anaerobic hyperthermophilic archaeonPyrococcus horikoshii. Acta Crystallographica Section F: Structural Biology Communications, 2013, 69, 719-722.	0.7	12
18	Solution structure of the chitin-binding domain 1 (ChBD1) of a hyperthermophilic chitinase from Pyrococcus furiosus. Journal of Biochemistry, 2014, 155, 115-122.	0.9	12

TSUTOMU NAKAMURA

#	Article	IF	CITATIONS
19	Crystallization and preliminary X-ray diffraction analysis of thioredoxin peroxidase from the aerobic hyperthermophilic archaeonAeropyrum pernixK1. Acta Crystallographica Section F: Structural Biology Communications, 2005, 61, 323-325.	0.7	10
20	Crystallization and preliminary X-ray diffraction analysis of a chitin-binding domain of hyperthermophilic chitinase fromPyrococcus furiosus. Acta Crystallographica Section F: Structural Biology Communications, 2005, 61, 476-478.	0.7	10
21	Alteration of molecular assembly of peroxiredoxins from hyperthermophilic archaea. Journal of Biochemistry, 2017, 162, 415-422.	0.9	8
22	Growth of Protein Crystals by Syringe-Type Top-Seeded Solution Growth. Crystal Growth and Design, 2011, 11, 1486-1492.	1.4	7
23	Amyloid fibril formation by the CAD domain of caspase-activated DNase. Biopolymers, 2005, 79, 39-47.	1.2	6
24	Crystallization and X-ray diffraction analysis of a catalytic domain of hyperthermophilic chitinase fromPyrococcus furiosus. Acta Crystallographica Section F: Structural Biology Communications, 2006, 62, 791-793.	0.7	6
25	Multiple crystal forms ofN,N′-diacetylchitobiose deacetylase fromPyrococcus furiosus. Acta Crystallographica Section F, Structural Biology Communications, 2015, 71, 657-662.	0.4	6
26	Substrate recognition of N,N′-diacetylchitobiose deacetylase from Pyrococcus horikoshii. Journal of Structural Biology, 2016, 195, 286-293.	1.3	6
27	Structural analysis and reaction mechanism of malate dehydrogenase from <i>Geobacillus stearothermophilus</i> . Journal of Biochemistry, 2021, 170, 97-105.	0.9	6
28	Growth of large protein crystals by a large-scale hanging-drop method. Journal of Applied Crystallography, 2010, 43, 937-939.	1.9	4
29	Heatâ€induced native dimerization prevents amyloid formation by variable domain from immunoglobulin lightâ€chain <scp>REI</scp> . FEBS Journal, 2017, 284, 3114-3127.	2.2	4
30	Application of chromosomal gene insertion into Escherichia coli for expression of recombinant proteins. Journal of Bioscience and Bioengineering, 2018, 126, 266-272.	1.1	4
31	Distinct molecular assembly of homologous peroxiredoxins from Pyrococcus horikoshii and Thermococcus kodakaraensis. Journal of Biochemistry, 2019, 166, 89-95.	0.9	4
32	Disassembly of the ringâ€ŧype decameric structure of peroxiredoxin from Aeropyrum pernix K1 by amino acid mutation. Protein Science, 2020, 29, 1138-1147.	3.1	4
33	Polyploid engineering by increasing mutant gene dosage in yeasts. Microbial Biotechnology, 2021, 14, 979-992.	2.0	4
34	NMR assignment of the chitin-binding domain of a hyperthermophilic chitinase from Pyrococcus furiosus. Journal of Biomolecular NMR, 2006, 36, 70-70.	1.6	3
35	Mass Spectrometric Analysis Using Ruthenium (II)-Labeling for Identification of Glycosyl Hydrolase Product. Bioscience, Biotechnology and Biochemistry, 2009, 73, 428-430.	0.6	3
36	Rebuilding Ring-Type Assembly of Peroxiredoxin by Chemical Modification. Bioconjugate Chemistry, 2021, 32, 153-160.	1.8	3

Tsutomu Nakamura

#	Article	IF	CITATIONS
37	Phosphoenolpyruvate carboxylase of Thermus sp.: role of a divergent glycine-rich region. Biotechnology Letters, 1997, 19, 335-340.	1.1	2
38	Thermostable and active phosphoenolpyruvate carboxylase from Thermus sp. even after proteolytic cleavage. Journal of Molecular Catalysis B: Enzymatic, 2002, 17, 215-222.	1.8	2
39	Increasing loop flexibility affords low-temperature adaptation of a moderate thermophilic malate dehydrogenase from <i>Geobacillus stearothermophilus</i> . Protein Engineering, Design and Selection, 2021, 34, .	1.0	2
40	Molecular characterization of recombinant phosphoenolpyruvate carboxylase from an extreme thermophile. Studies in Surface Science and Catalysis, 1998, 114, 605-608.	1.5	1
41	Crystallization and preliminary crystallographic analysis of a putative glucokinase/hexokinase from Thermus thermophilus. Acta Crystallographica Section F: Structural Biology Communications, 2011, 67, 1559-1562.	0.7	1
42	Crystal structure of acetylxylan esterase from <i>Caldanaerobacter subterraneus</i> subsp. <i>tengcongensis</i> . Acta Crystallographica Section F, Structural Biology Communications, 2021, 77, 399-406.	0.4	1
43	Identification of the Region Responsible for Fibril Formation in the CAD Domain of Caspase-Activated DNase. Journal of Biochemistry, 2005, 138, 815-819.	0.9	О